Experience with the Johnson–King turbulence model in a transonic turbine cascade flow solver

N. B. Wood
National Power Technology and Environmental Centre, Leatherhead, UK

Experience is described of the application of the Dawes Navier–Stokes solver to a turbine test case involving shock–boundary-layer interaction. Modifying the implementation of the algebraic eddy-viscosity turbulence model gave improved agreement between the predictions and the experimental results.

In order to improve the predictions still further, the nonequilibrium turbulence model of Johnson and King was incorporated into the code. This gave limited further improvement in the overall loss prediction, but the base pressure prediction was not improved. Only a minor shock-induced separation was predicted, compared with the increasing major separation observed in cascade tests with increasing outlet Mach number, although it is necessary to be aware of the possible differences between the real test flow and the two-dimensional steady flow that was modeled.

Better prediction of the test flow may require the incorporation of higher-order turbulence models, in which the physics of the flow is more fully represented. Additionally, three-dimensional and unsteady capability may be needed.

Keywords: fluid dynamics; turbulence models; compressible flow; shock–boundary-layer interaction

Introduction

The advent of so-called *Navier–Stokes solvers* has already made a considerable impact on the conduct of research and development in fluid dynamics. Greater understanding of fluid-flow phenomena is already being achieved, for example in computing flow features that are not readily accessible by experimental means, and reference is sometimes made to the *numerical wind tunnel*. However, the analogy with the wind tunnel is not exact, since computation requires an approximate mathematical model of the physical process being simulated, whereas in the wind tunnel a real model flow is created, albeit one that differs from the full-scale flow as a result of wall interference. Differences of scale may also require artificial means to induce the wind-tunnel flow to behave more like that in full scale. Computational means are now being applied to aid the application of model flow results to full-scale situations. Nevertheless, just as it is necessary to understand the limitations and inaccuracies involved in wind-tunnel simulations, so the same is true of computational fluid dynamics. In particular, it is necessary to be able to gain confidence in the latter by demonstrating the ability to compute the important features of real test flows.

In practice, there are various factors that limit the ability of Navier–Stokes codes to compute flows correctly, especially turbulent flows. For example, the discretization method adopted and the numerical dissipation incorporated can affect both the stability and accuracy of the computation. The implicit finite-difference time-marching solver used for the present study was developed by Dawes,[1] based on the methods of Beam and Warming[2] but with modified numerical dissipation and with a more efficient solution method. The accuracy of the basic algorithm is second order in space and first order in time. However, the time accuracy is not directly relevant in the present code, which is marched in time to a steady-state solution.

Before discretization, the Navier–Stokes equations have to be simplified, usually by time-averaging the turbulent fluctuation terms in the equations. This leads to the appearance of the Reynolds stresses, averaged turbulence-related terms that must be modeled to achieve closure of the equation set. The terms have to be approximated, and the different ways of doing this form the general topic of turbulence modeling. There is a big range of possibilities in turbulence modeling, but among the popular methods for engineering computations are those that give effective eddy viscosity. Some more advanced techniques involve modeling of the Reynolds stresses, and progress is being made with simulation of the large eddies. In the latter case, computer limitations mean that the calculation grid cannot be made small enough to model the effects of the smallest turbulent eddies, so combinations of grid and turbulence models must be put together that will adequately model the flow to be computed. We are concerned here with eddy-viscosity methods in which the grid is required to be fine enough in the boundary layer for profiles of relevant parameters to be defined adequately. The eddy viscosity, which is a property of the flow rather than the fluid, may be provided by algebraic means via estimation of characteristic turbulence length and velocity scales, but these are local methods that do not take into account the effects of streamwise flow development on turbulence structure. This may be achieved by more complex means involving ordinary or partial differential turbulence transport equations, but there are many flow situations where these methods are still inadequate.

A feature of particular importance in considering the performance of high-speed turbines is the occurrence of separated flows and the ability to predict and control them.

One phenomenon that can induce flow separation is a shock

Address reprint requests to Dr. Wood at the National Power Technology and Environmental Centre, Leatherhead KT22 7SE, UK.

Received 4 January 1989; accepted 8 October 1990

wave impinging on a bounding surface. The fluid boundary layer will be retarded by the adverse pressure gradient imposed by the shock wave, and this may result in flow separation. The occurrence of the separation and its extent will depend on the strength of the shock and the state of the boundary layer. This process of shock–boundary-layer interaction has been widely studied in the aircraft industry, where it has major importance for both economic and stability reasons.

Transonic and supersonic flows occur also in the downstream stages of low pressure (LP) turbines where, therefore, shock-induced separation can arise, with associated economic penalties.

The two-dimensional (2-D) Navier–Stokes implicit solver developed by Dawes[1] incorporates the equilibrium algegraic eddy-viscosity turbulence model of Baldwin and Lomax.[3] This was used as the starting point in an investigation into the ability of this class of program to calculate shock–boundary-layer interaction. Further results were then obtained using a method in which a turbulence transport equation is introduced to take some account of flow history. The experimental results described in the following section offered a challenging test case that, it was expected, would provide a severe test of the calculation methods.

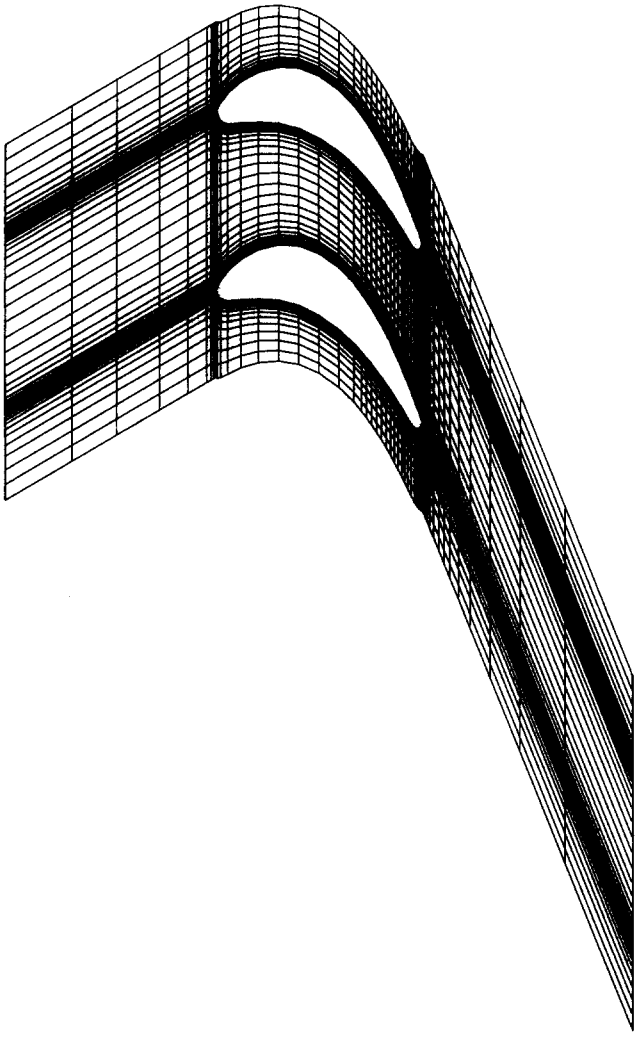

Figure 1 VKI-1 turbine blade profile and computation grid (fineness reduced to aid clarity)

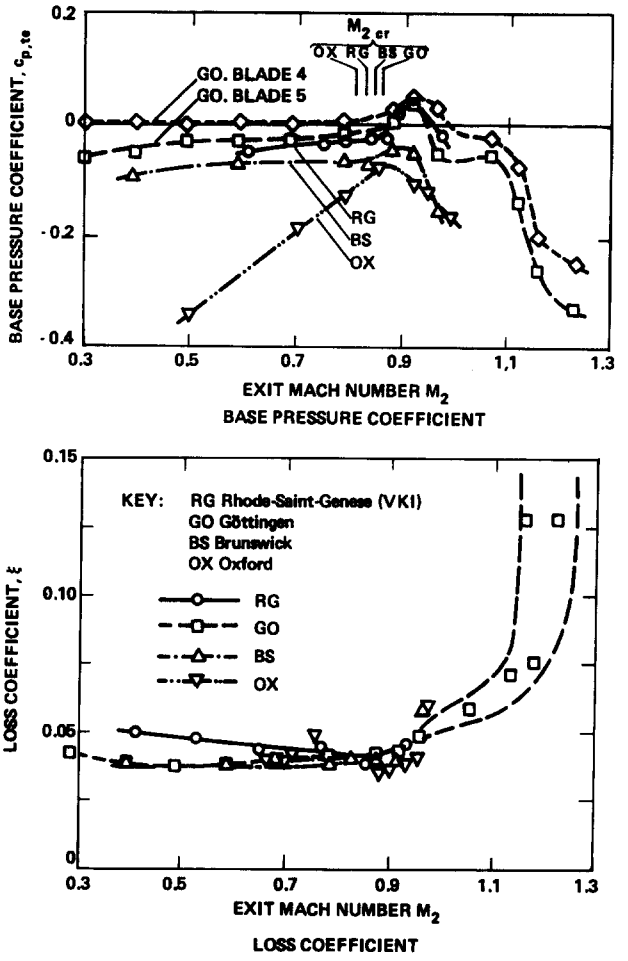

Figure 2 Variation of measured energy loss coefficient and base pressure coefficient with exit Mach number at near-zero incidence (inlet angle = 30°)[4]

A suitable test case

A particularly interesting test case that has appeared in the literature is the von Karman Institute (VKI) gas turbine blade (Figure 1) tested over a range of transonic conditions in four different wind tunnels, at DLR Brunswick, DLR Göttingen, Oxford University, and the von Karman Institute.[4]

Actually, results from only one of the facilities (at Göttingen) extended to supersonic Mach numbers. With supersonic Mach numbers, these results showed the base pressure coefficient decreasing markedly and the energy loss coefficient increasing at a rate greater than that owing to the base pressure alone, as shown in Figure 2. Further, the shock-induced separated flow became increasingly unsteady with increasing outlet Mach numbers. Associated with the increasing Mach number, of course, would be a shock of increasing strength generated at the pressure surface side of the trailing edge and impinging on the suction surface where it would be expected to have a strong effect on the boundary layer. This was shown in a series of schlieren photographs published in an earlier report on the Göttingen tests.[5] The Reynolds number was approximately 8×10^5.

Such a flow structure is typical of the end stages of steam turbines, although the trailing edge is relatively thicker in this gas turbine geometry.

Initial results with the algebraic eddy-viscosity model

The first promising results were obtained for the VKI blade on the 91 (quasi-orthogonals) × 51 (quasi-streamlines) grid after initial results on a 50 × 21 grid had given loss coefficients two to three times those measured. (Figure 1 has a coarse 52 × 31 grid to aid clarity of presentation.) The general features of the flow field (shock waves and wake direction), shown by computed Mach number contours, were in good agreement with Lehthaus'[5] schlieren photographs for averaged exit Mach numbers up to 1.2, but above this condition the experimental cascade exhibited flow separation from the suction surface, which was not detectable in the computation results.

Figure 3 shows some predicted results for the energy loss coefficient ($\xi = 1-(u/u_{is})^2$, where u and u_{is} are the effective uniform cascade exit velocities for actual and isentropic flows, respectively) and base pressure coefficient ($c_{p,b}=(p_b-p_{exit})/q$, where q is the mean dynamic pressure at exit), for a range of outlet Mach number from just below unity to 1.35. The dashed lines here and in Figures 6 and 7 are based on the dashed lines of Figure 2 and represent the bounds of the main body of experimental data. As can be seen, the trend of base pressure is downwards with increasing Mach number, but the base pressure coefficient does not fall as rapidly as indicated by the experiments. The loss coefficient shows an increasing trend with increasing supersonic Mach number, but it is overpredicted at sonic outflow and does not increase to the extent shown by measurements. There are aspects of the grid that require further comment, but it is the turbulence model in the program that needs to be considered first, for reasons that will become apparent.

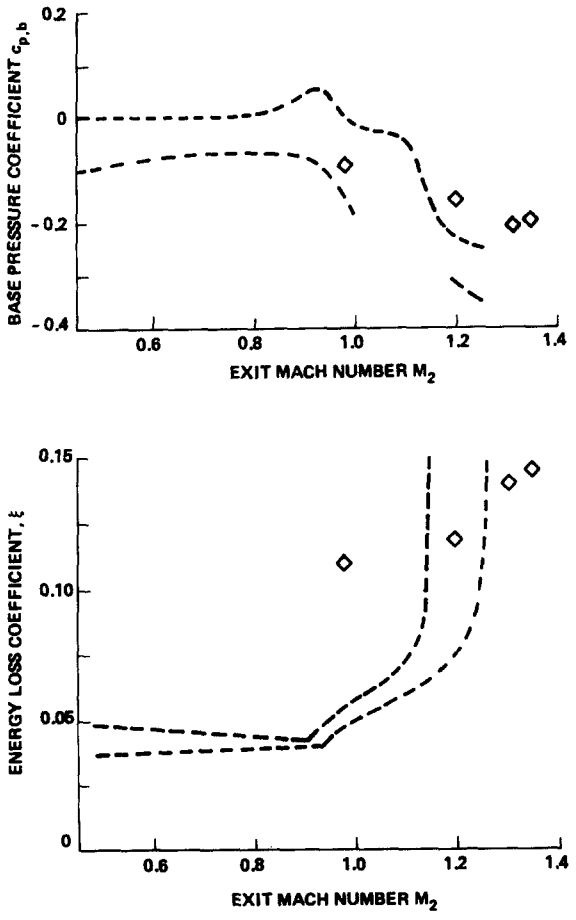

Figure 3 Variation of energy loss coefficient and base pressure coefficient predicted by initial version of the program (91 × 51 grid)

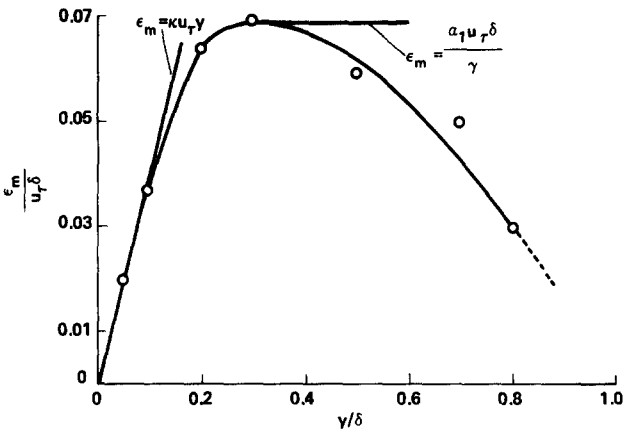

Figure 4 Form of the turbulent eddy-viscosity distribution across the boundary layer, shown as dimensionless kinematic viscosity[7]

The algebraic eddy-viscosity model and its implementation

The viscous terms in the Navier–Stokes equations as solved in the Dawes code[1] are time averaged, and the shear stresses are modeled via an algebraic eddy-viscosity model based on the method of Baldwin and Lomax.[3] This method was itself based on the eddy-viscosity boundary-layer model of Cebeci and Smith,[6] but with a technique incorporated to avoid having to determine explicitly the boundary-layer thickness. This allows the method to be used in flows like those in turbomachinery, where there are strong velocity gradients outside the boundary layer that make it difficult to locate the outer edge and hence to obtain a realistic distribution of eddy viscosity.

The Cebeci–Smith model is a two-layer formulation in which the length scale for the inner layer is proportional to the distance from the surface. For the outer layer the length scale varies with the boundary-layer thickness. Baldwin and Lomax define the outer length scale instead via the distance from the surface of the maximum value of a velocity scale (vorticity × length scale) parameter or of a wake parameter. The form of the equilibrium eddy-viscosity distribution (derived from measurements, e.g., Klebanoff[7]) on which these two-layer models are based is shown in Figure 4. The decline in eddy viscosity towards the outer part of the boundary layer results from the intermittency.

Improvements to the implementation

As can be seen in Figure 4, the inner-layer eddy viscosity increases with distance from the surface, while in the outer layer it is represented by a constant multiplied by the intermittency function, γ. Baldwin and Lomax, following Cebeci and Smith, suggest changing from the inner to the outer law at the smallest distance from the wall at which the values from the two formulations are equal.

In practice, of course, since the parameters are stored on a finite-difference grid, they will not generally be equal at any point. Therefore, it is important to avoid the pitfall of setting the crossover point where the inner ν_t is greater than the outer ν_t. This will give a local false peak in the distribution that can

cause problems in the maximum-seeking routines invoked later, and so it has been avoided.

The inner eddy viscosity is given in the Baldwin and Lomax formulation by

$$(\nu)_i = l^2|\omega| \tag{1}$$

where l is the length scale and ω is the vorticity ($\omega = \partial u/\partial y - \partial v/\partial x$ in two dimensions). Usually the inner eddy viscosity is taken to be proportional to the shear rate $(\partial u/\partial y + \partial v/\partial x)_w$ where the subscript w signifies wall or boundary-layer coordinates, which are required for calculating the eddy viscosity; for the boundary-layer approximation, this is taken to be $(\partial u/\partial y)_w$. Presumably the reason why Baldwin and Lomax specify vorticity is that this parameter is independent of the orientation of the grid and can be taken as approximately equal to $(\partial u/\partial y)_w$ in thin shear layers. With the use of the H grid shown in Figure 1, it is important to take care that the term $\partial v/\partial x$ is computed as a true partial derivative.

For the purposes of the current investigation, ω has been replaced by $(\partial u/\partial y)_w$, i.e., the approximate shear rate in boundary-layer coordinates, which is considered to be a better approximation to the shear rate than is the vorticity.

The outer velocity scale, F, defined by Baldwin and Lomax and whose maximum, F_{max}, is sought in the process introduced to avoid searching for the outer edge of the boundary layer, is

$$F = y|\omega|[1 - \exp(-y^+/A^+)] \tag{2}$$

where y^+ is $yu^\times/\nu$, $u^\times$ being the friction velocity and A^+ the dimensionless van Driest damping parameter (an empirical constant).

Since the parameter F can have large values beyond the (unknown) boundary-layer edge, it is necessary to apply a cutoff on ω according to the following algorithm:

$$\omega_{cut} = \omega_{max} - C_{cut}(\omega_{max} - \omega_{min}) \tag{3}$$

and ω is set to zero if it is less than ω_{cut}. This is not specified in the Baldwin–Lomax paper, but appears to be required by the method.

ω_{max} and ω_{min} are respectively the maximum and minimum values of ω occurring between the wall and the midstreamline of the blade passage. The results in Figure 3 were obtained with the code as received, i.e., with $C_{cut} = 0.90$, and the effect of this parameter on eddy viscosity distribution is shown in Figure 5. With $C_{cut} = 0.90$, the turbulent eddy viscosity is computed to be of similar order to the molecular (i.e., laminar) viscosity. However, if no cutoff is applied, the program may compute distributions of eddy viscosity that fluctuate in the streamwise direction between plausible and implausible values and that give boundary layers extending to the center streamline. However, it can be seen that the original C_{cut} gives a very unlikely looking eddy-viscosity profile. Increasing the value of C_{cut} to 0.95 produces a much more believable profile and increases the distance from the surface y_{max} of F_{max} by an order of magnitude. Increasing C_{cut} further to 0.99 still produces a plausible profile, with a further 50% increase in y_{max} and a doubling of the maximum eddy viscosity, but it occasionally gives similar problems to those that arose when there was no cutoff. Nevertheless, 0.99 gives the nearest practical approach to the case with no cutoff (i.e., C_{cut} equal to unity), with similar results for most of the flow field, so this value was used subsequently. Overall, the need for this cutoff was an unsatisfactory feature of the Baldwin–Lomax procedure. Figure 5 also shows the false local peak in the distribution that occurred at the junction between the inner and outer eddy viscosities in the original version of the code.

Finally, it was pointed out by Visbal and Knight[8] that the velocity scale F of Baldwin and Lomax, mentioned earlier, can have genuine double peaks, and that it is the outer of the two that should be sought when this happens. This recommendation was implemented for all the results that follow.

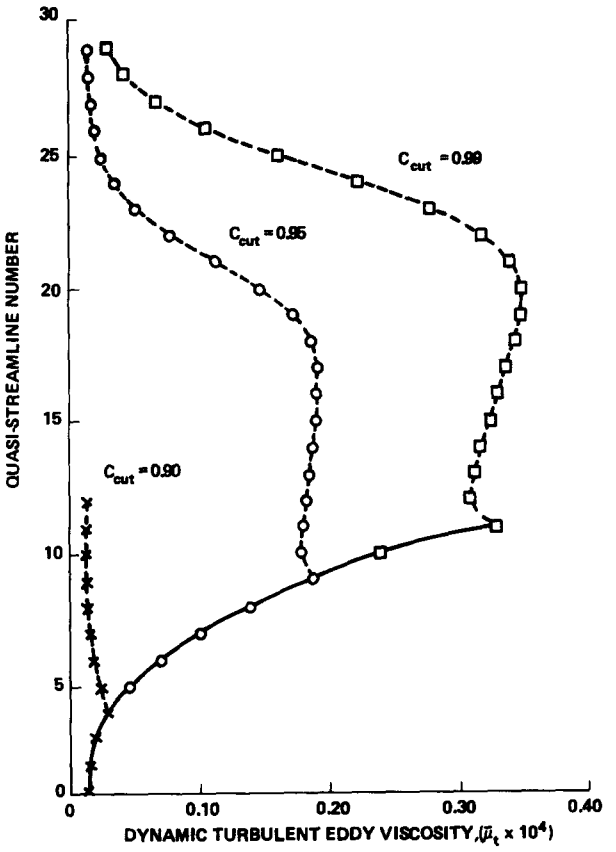

Figure 5 Effect on eddy-viscosity distribution of applying a cutoff on the boundary-layer shear rate

Results with improved implementation

Figure 6 shows the changes in the results obtained following the modifications to the program discussed in the previous section. With the same 91×51 grid used before, the loss coefficients obtained were in extremely good agreement with the experimental results over the Mach number range unity to 1.25, although beyond this the loss was underpredicted, presumably because the major suction surface separation seen in the experiments was not computed. Moreover, the agreement on base pressure coefficients was worsened.

With only 51 quasi-streamlines (q.s.'s) the q.s. nearest the surface could be outside the viscous sublayer for stations near the leading edge, which is undesirable in algebraic eddy-viscosity methods. Whilst there was a routine in the program to deal with this situation, it is more satisfactory to refine the grid to ensure that the boundary layer is well defined. Therefore, the number of q.s.'s was increased to 91, which had the effect of improving the profile definition and of keeping the q.s. adjacent to the boundary entirely within the sublayer. Further, the disposition of the quasi-orthogonals (q.o.'s) was altered to give better definition of the profile leading edge and to give a smoother transition from coarse to fine mesh in the supersonic zone, where shock waves are expected. This gave a mesh of 93×91, for which the results are shown in Figure 6. It can be seen that, despite refining the mesh to allow good definition of the boundary-layer profile, the loss level increased near the

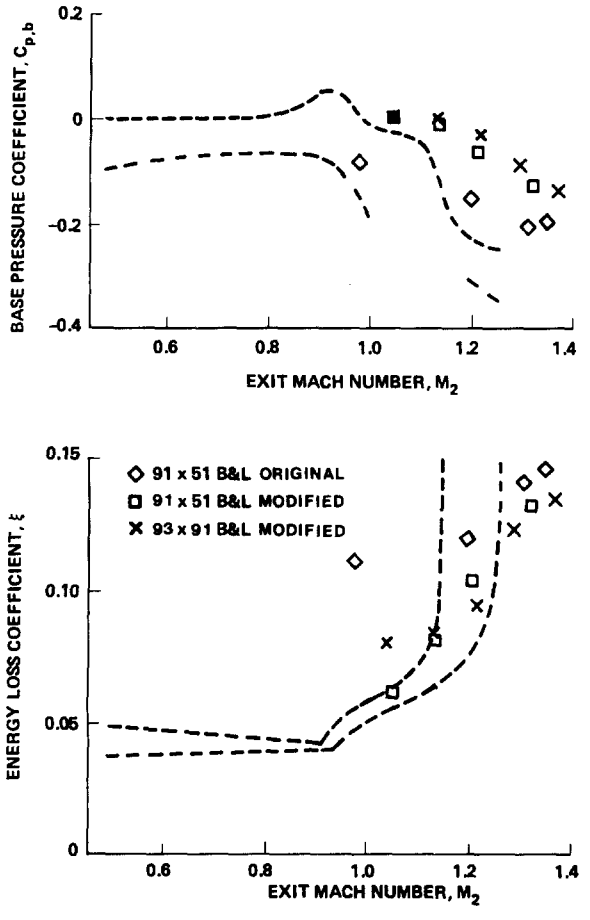

Figure 6 Variation of energy loss coefficient and base pressure coefficient predicted with the Baldwin–Lomax (B&L) turbulence model

condition of sonic outflow, so that the overall agreement on variation of loss with Mach number was slightly worsened.

It was decided to leave the Baldwin and Lomax method at this point, since it would always suffer the limitation of being an equilibrium turbulence model, and to test a model that takes some account of flow history, i.e., the streamwise development of the turbulence structure.

Improved turbulence models

The most popular turbulence transport model for some years has been the Jones and Launder[9] k–ε two-equation system, involving partial differential equations for the turbulence kinetic energy, k, and the dissipation, ε. If these two equations were solved simultaneously with the main flow equations, as is sometimes done, a new solver would be required. However, they could be solved separately, since their only interaction with these equations is to supply turbulent eddy-viscosity distributions.

A boundary-layer method that is used extensively in the aircraft industry on shock–boundary-layer interaction studies is the lag-entrainment momentum integral technique.[10] This is derived from the turbulence kinetic energy equation of Bradshaw et al.[11] Wood was beginning a study to use this as the basis for a simple model to be incorporated in a Navier–Stokes solver when the boundary-layer method of Johnson and King[12] appeared in a version applied to a Navier–Stokes solver.[13] This is, in effect, an update of the Cebeci–Smith boundary-layer model using just such a method. Therefore, it has been used as the basis for a test in the present application.

The Johnson and King turbulence model

In the paper by Johnson and King,[12] the new model was tested in a boundary-layer calculation and compared with results from the Cebeci and Smith method. Subsequently, Johnson[13] incorporated the model into MacCormack's[14] semi-implicit Navier–Stokes solver and was able to compare the results with both the Cebeci–Smith and the Jones–Launder[9] k–ε model, which were options in the program. The new model was reported to give extremely good agreement with experimental pressure distributions, with shock position predicted better than with the other two models, and the predicted distributions of Reynolds shear stresses were better. However, the value of a scaling parameter σ had to be limited downstream from the shock to achieve stability, as discussed in the next section. If the value of σ remained at this set limit at the conclusion of the computation, as it appeared to be in King's paper, the solution in this region obviously should not have been considered as converged.

In an independent study, Benay et al.[15] compared predictions of shock–boundary-layer interaction using several algebraic eddy-viscosity models, the Jones–Launder k–ε, and an algebraic stress model (ASM) like that of Hanjalic and Launder.[16] An inverse boundary-layer technique was used in which the displacement thickness distribution obtained experimentally was imposed. This allows the boundary-layer method to be used with separated flows, but it places artificial limitations on the comparison. Nevertheless, it was interesting to note that, with this constraint, the two turbulence transport models gave the best agreement with the three experimental test cases, comprising one incipient separation and two separated flows, on the basis of pressure distribution and distributions of mean velocity and Reynolds shear stress. However, the results given by the Johnson–King method were not significantly different from the last two, except that a longer separation bubble was predicted in one case.

The principal feature of the Johnson–King model is the reduction of the turbulence kinetic energy equation from a partial differential equation (PDE) to an ordinary differential equation (ODE) by solving for maximum k and then, using the result that the ratio of k to Reynolds shear stress is broadly constant across the shear layer,[11] substituting the maximum of the latter parameter. In fact, the variable is $(-\overline{u'v'})_{max}$ rather than $(-\rho\overline{u'v'})_{max}$ and is used in an analogous way to the square of the friction velocity. Following Johnson and King, and others, $(-\overline{u'v'})$ will be referred to as Reynolds shear stress in the remaining discussion. Finally, the equation is linearized by solving for the inverse square root of $(-\overline{u'v'})_{max}$ along s, the near-streamwise locus of the maximum value.

The ODE is, then,

$$\frac{dg}{ds}=\frac{a_1}{2\bar{u}_m L_m}\left[\left(1-\frac{g}{g_{eq}}\right)+\frac{C_{dif}L_m}{a_1\delta[0.7-(y/\delta)_m]}\,|1-\{\sigma(s)\}^{1/2}|\right] \qquad (4)$$

where

$$g=(-\overline{u'v'})_m^{-1/2}$$

The length scale, L_m, is given by

$$L_m=0.4y_m \qquad y_m/\delta\leq 0.225,$$

$$L_m=0.09\delta \qquad y_m/\delta>0.225,$$

g_{eq} is the equilibrium value of $g(s)$, and C_{dif} is a diffusion

modeling constant. The subscript m refers to the position where $(-\overline{u'v'})$ has a maximum value.

The result is used in a two-layer eddy-viscosity model, which, following further development by Johnson,[13] is as follows:

$$\nu_{ti} = D^2 \kappa y (-\overline{u'v'})_m^{1/2} \tag{5a}$$

$$\nu_{to} = \sigma(s)(0.0168 u_e \delta^* \gamma) \tag{5b}$$

$$\nu_t = \nu_{to}\{1 - \exp(-\nu_{ti}/\nu_{to})\} \tag{5c}$$

where

$$D = 1 - \exp\{-(-\overline{u'v'})_m^{1/2} y/(\nu A^+)\} \tag{5d}$$

The function $\sigma(s)$ is a scaling parameter on the outer eddy viscosity that matches the algebraic distribution with the maximum value given by the ODE. Therefore, the method proceeds with an iteration between the algebraic distribution generated by the flow and the ODE solution from the previous timestep, viz.,

$$\nu_t = \frac{-\overline{u'v'_m}}{\partial \bar{u}/\partial y_w} \tag{6}$$

and the ODE solution obtained in the current timestep.

The method was developed for external flows where the Cebeci–Smith method would be applicable, and it is necessary to consider its adaptation to internal flows, taking account of the Baldwin–Lomax conversion of the Cebeci–Smith method and of experience of the working of the Johnson–King model in practice.

Adaptation of the new turbulence model to the cascade flow

The first point to notice is that, apart from the parameter $\sigma(s)$, the outer eddy viscosity follows the Cebeci–Smith formulation. Therefore, for the present application the Baldwin–Lomax outer formulation has been adopted, but multiplied by $\sigma(s)$, i.e.,

$$\nu_{to} = \sigma(s)(0.0168 C_{CP} F_{WAKE} \gamma) \tag{5e}$$

where C_{CP} is an additional constant and F_{WAKE} is the product of a velocity scale and a length scale, usually F_{max}, and the distance from the surface of this maximum value, y_{max}.

This avoids the specification of boundary-layer thickness, which appears also in the outer length scale L_m and in a turbulence diffusion term in one of the coefficients of the ODE. Taking the Baldwin–Lomax formulation of the intermittency function γ and comparing it with the Cebeci–Smith formulation gives $\delta \sim 3.3 y_{max}$, where y_{max} is the length scale referred to above. This approximation is considered to be of similar order to the approximations used to derive these two parameters.

The Johnson–King procedure was followed largely as recommended by the authors, although some changes were required to achieve stability. As suggested, the procedure was started from a converged equilibrium turbulence model solution, in this case that of the Baldwin–Lomax model. Initially the Johnson–King equilibrium model ($\sigma = 1.0$, with $-\overline{u'v'_m}$ evaluated from the Baldwin–Lomax solution) was substituted and run for several timesteps. After convergence was established in this mode, the solution of the ODE was used to update σ via the iteration method described by Johnson.[13] However, the recommended procedure involved attempting to reconcile the values of maximum Reynolds stress obtained (1) via direct search across the existing profile and (2) as the solution of the ODE, by updating the value of σ. When the maximum value of Reynolds stress occurred in the inner layer, it could prove impossible to obtain a converged value of σ. Therefore, in addition to updating σ, the maximum Reynolds stress given by the ODE was substituted into the relation for the inner-layer eddy viscosity. Even with this modification, the process for updating σ could sometimes fail to converge, so Johnson's recommendation to set an upper limit to σ of 4.0 was followed. His recommendation to set an even tighter limit downstream from the shock was not followed because this would further limit the validity of the solution. Johnson's test case was a cylindrical body axially aligned with the flow in a transonic wind tunnel, the shock being generated by a bulge in the surface. Therefore, the flow ahead of the shock was axially uniform and no region of accelerating flow, like that in a turbine cascade, existed.

In the present application, it was the accelerating parts of the flow that caused the most difficulty, both ahead of the shock on the pressure surface and especially in the expansion around the trailing edge on the suction surface. At the time of this writing, a stable solution has not been obtained for the latter region, and the results given were obtained with the Baldwin–Lomax model applied to the pressure surface. This is unsatisfactory, but there are further unsatisfactory features of the method, as discussed below. Nevertheless, the Johnson–King method has been used through the shock–boundary-layer interaction region, which was the object of this study. Chokani[17] also experienced instabilities in accelerating flows when using the method in a different application. He believed that the fault lay in the approximate terms introduced by Johnson and King

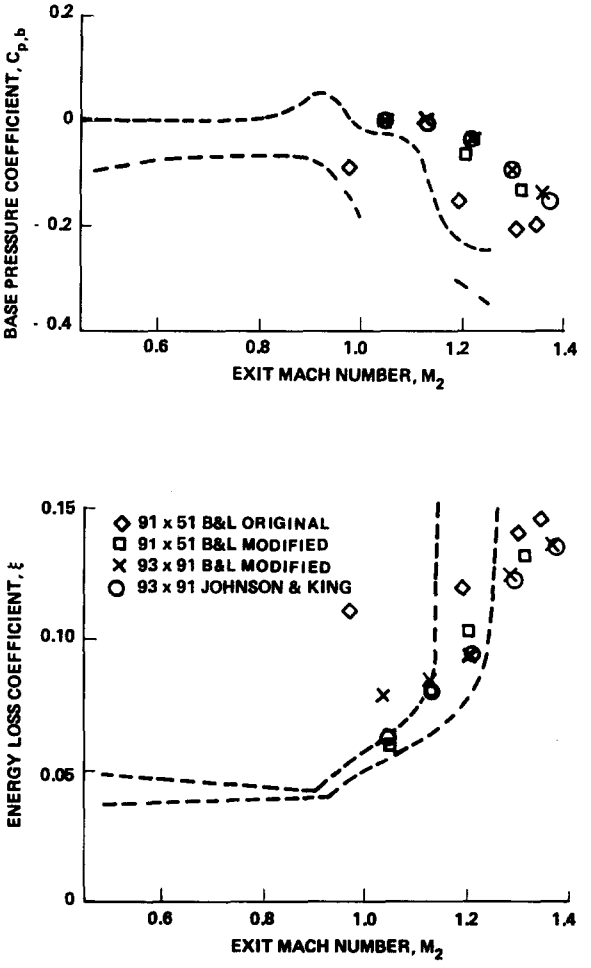

Figure 7 Variation of energy loss coefficient and base pressure coefficient predicted with the Baldwin–Lomax (B&L) and Johnson–King turbulence models

into the turbulence energy equation,[4] and considered that experimentation with alternative terms, such as those introduced by Green et al.,[10] might bear fruit. However, the method relies on an inconsistency, which is the attempt to alter the magnitude of an equilibrium distribution to match the value of a single point in a nonequilibrium distribution, which in principle may be different in form. Moreover, the principle of the similarity in the distributions of turbulence kinetic energy and Reynolds stress, on which the method relies, is also dependent on the boundary layer being near equilibrium.

Results with the Johnson and King turbulence model

Figure 7 shows the loss coefficients obtained from a computation on a 91×93 grid, as used in the previous example. It can be seen that the main effect was to improve the prediction for near-sonic outflow, with overall levels very similar to those obtained with the Baldwin–Lomax model on the finer grids. The base pressure results were similar to those obtained on the 93×91 grid with Baldwin–Lomax.

Figures 8 and 9 show Mach number contours computed at isentropic exit Mach numbers of 1.10 and 1.30 (1.06 and 1.22 actual). The development of the passage shock with increasing Mach number can be seen, but the large suction surface separation observed in the cascade tests was not computed.

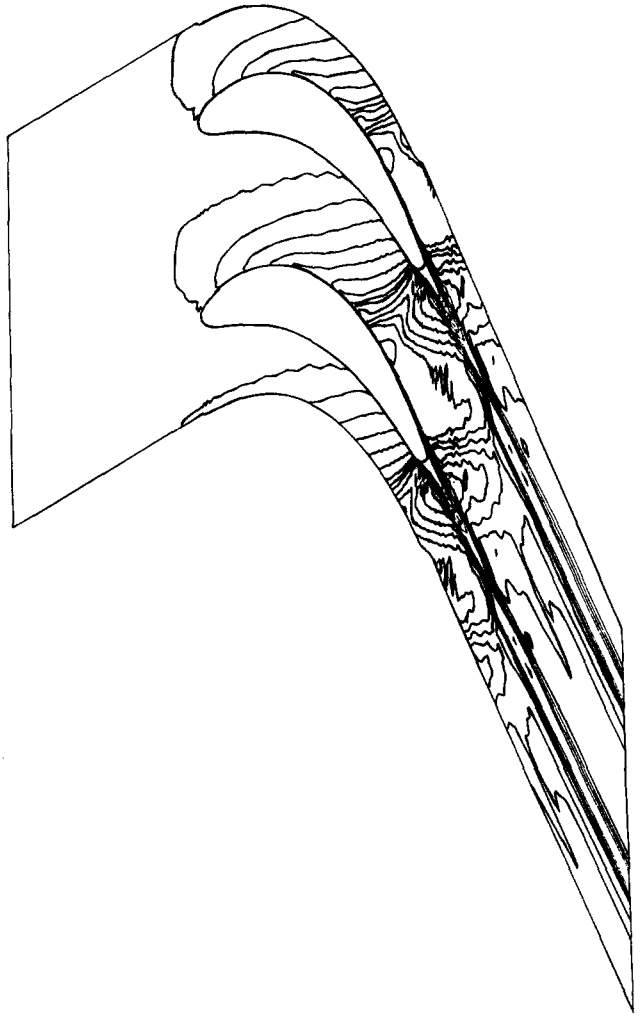

Figure 8 Mach number contours on 93×91 grid. Isentropic exit Mach number = 1.10 (Johnson–King turbulence model)

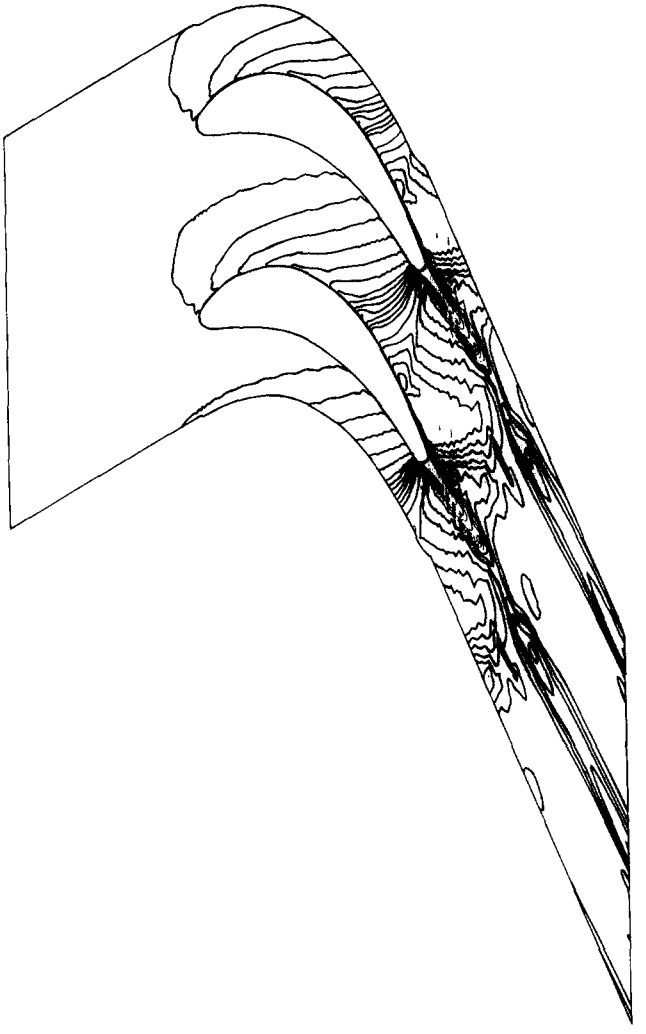

Figure 9 Mach number contours on 93×91 grid. Isentropic exit Mach number = 1.30 (Johnson–King turbulence model)

Small separation regions were computed at higher Mach numbers. The shocks are captured typically within three cells, but the skewed cells inherent in the H grid give rise to considerable streamwise smearing unless the shock is aligned with the grid. Therefore, while the algorithm gives good shock capture, its performance is limited in the present implementation by being allied to a fixed H grid. Clearly, introduction of an adaptive grid is desirable to compute flows in which shock waves are formed.

It should be pointed out that validation of two-dimensional (2-D) flow solvers against experimental turbomachinery cascade test cases brings special problems, as pointed out by Fottner.[18] In comparing results from nominally 2-D cascade tests, particularly where the trailing edges are blunt, there may be significant global differences between the test flow and the computed flow; for example:

- the test flow may not be truly 2-D;
- the computed flow converges to a steady solution, while the wake from a blunt trailing edge contains a cyclic component for most flow regimes;
- the test flow considered here became more unsteady with increasing exit Mach number.

These features could be investigated by modeling the test flow

with a three-dimensional (3-D) computation in which both steady and unsteady solutions are possible.

As mentioned in the previous section, there have been problems with the stability of the Johnson–King method when applied to the expansion around the trailing edge, so the results presented in Figure 7 were obtained with the pressure surface and trailing-edge conditions computed via the Baldwin–Lomax method. Further work is required to improve the ability of the Johnson–King model to cope successfully with flows of this type. However, it is likely that the method is restricted to near-equilibrium flows, and the time might be better spent on a higher-order model. For example, a two-equation model from which the eddy-viscosity distribution may be derived should be more stable and, while the predictions of Reynolds stresses may in some cases be little better than those obtained with the Johnson–King model, the profiles would be less constrained. Moreover, the former class of model incorporates more of the physics of the problem and should be generally more reliable.

Conclusions

Experience has been described on the application of the Dawes Navier–Stokes solver[1] to a transonic turbine cascade test case involving shock–boundary-layer interaction. Improved implementation of the Baldwin–Lomax[3] algebraic turbulence model, coupled with grid refinement, gave predictions that were in better agreement with the experimental results than initial computations.

In an attempt to improve the predictions still further, the nonequilibrium turbulence model of Johnson and King,[12] employing a single ODE for the streamwise evolution of the peak turbulence kinetic energy and algebraic laws for its transverse distribution and for the dissipation, was incorporated into the code. Although there appears to be a fundamental inconsistency in this model, it gave limited further improvement in the overall loss prediction, but the base pressure prediction was not improved. Moreover, with increasing exit Mach number only a limited shock-induced separation was predicted, compared with the increasing major separation observed in cascade tests. However, it is necessary to maintain awareness of the differences between the real test flow and the 2-D steady flow that was modeled.

Necessary to the use of both the Baldwin–Lomax and the Johnson–King models were stops in the computation, which were required to prevent nonphysical results in the former and instability in the latter method. The use of the stop in the Johnson–King model, in the manner recommended by Johnson,[13] means that valid solutions cannot always be obtained downstream of shock waves. For the case presented here, which represents quite a severe test, the Johnson–King model was not stabilized on the pressure surface by the authors' recommended procedure. It is suggested that the Johnson–King model is suitable only for flows where the boundary layer remains near equilibrium.

Better prediction of the present test flow will require the incorporation of higher-order turbulence models, in which the physics of the flow is more adequately represented. Additionally, 3-D and unsteady capability may be needed.

Acknowledgment

The work was carried out at the National Power Technology and Environmental Centre, Leatherhead, UK (formerly Central Electricity Research Laboratories), and the article is published by permission of National Power plc.

References

1 Dawes, W. N. Efficient implicit algorithm for the equations of 2-D viscous compressible flow: application to shock–boundary interaction. *Int. J. Heat Fluid Flow*, 1983, **4**, 17–26

2 Beam, R. M. and Warming, R. F. On the construction and application of implicit factored schemes for conservation laws. *SIAM-IAS Proc.*, 1978, **11**, 85–129

3 Baldwin, B. S. and Lomax, H. Thin layer approximation and algebraic model for separated turbulent flows. AIAA Paper 78-257, 1978

4 Kiock, R., Lehthaus, F., Baines, N. C., and Sieverding, C. H. The transonic flow through a plane turbine cascade as measured in four European wind tunnels. *J. Eng. G T Power*, 1986, **108**, 277–284

5 Lehthaus, F. Experimental investigations into a gas turbine rotor cascade with blade profile VKI-1; Part I: Measurements made in the outlet flow field and schlieren photographs. DFVLR-AVA Report No 251 74 A 48, 1975 (Translation Ref 7323)

6 Cebeci, T. and Smith, A. M. O. *Analysis of Turbulent Boundary Layers*, London, Academic Press, 1974

7 Klebanoff, P. S. Characteristics of turbulence in a boundary layer with zero pressure gradient. NACA TN 3178, 1954

8 Visbal, M. and Knight, D. The Baldwin–Lomax turbulence model for two-dimensional shock-wave/boundary-layer interactions. *AIAA J.*, 1984, **22**, 921–928

9 Jones, W. P. and Launder, B. E. The prediction of laminarization with a two-equation model of turbulence. *Int. J. Heat Mass Transfer*, 1972, **15**, 301–314

10 Green, J. E., Weeks, D. J., and Brooman, J. W. F. Prediction of turbulent boundary layers and wakes in compressible flow by a lag-entrainment method. ARC R&M No. 3791, 1973

11 Bradshaw, P., Ferris, D. H., and Attwell, N. P. Calculation of boundary-layer development using the turbulent energy equation. *J. Fluid Mech.*, 1967, **28**, 593–616

12 Johnson, D. A. and King, L. S. A mathematically simple turbulence closure model for attached and separated turbulent boundary layers. *AIAA J.*, 1985, **23**, 1684–1692

13 Johnson, D. A. Transonic separated flow predictions with an eddy-viscosity/Reynolds-stress closure model. *AIAA J.*, 1987, **25**, 252–259

14 MacCormack, R. W. A numerical method for solving the equations of compressible viscous flow. *AIAA J.*, 1982, **20**, 1275–1281

15 Benay, R., Coet, M. C., and Délery, J. Validation de modèles de turbulence appliqués à l'interaction onde de choc-couche limite transsonique. ONERA TP No 1986-173, 1986

16 Hanjalic, K. and Launder, B. E. A Reynolds stress model of turbulence and its application to thin shear flows. *J. Fluid Mech.*, 1972, **52**, 609–638

17 Chokani, N. Private communication, Cambridge University Engineering Dept., 1988

18 Fottner, L. Overview on test cases for computation of internal flows in turbomachines. ASME Paper 89-GT-46, 1989